



1 Assessing local impacts of the A.D. 1700 Cascadia earthquake and tsunami using tree ring growth  
2 histories: A case study in South Beach, Oregon, U.S.A.

3 Robert P. Dziak<sup>1</sup>, Bryan A. Black<sup>2</sup>, Yong Wei<sup>3</sup>, and Susan G. Merle<sup>4</sup>

4 <sup>1</sup>NOAA/Pacific Marine Environmental Laboratory, Newport, Oregon, 97365 U.S.A.

5 <sup>2</sup>Laboratory of Tree-Ring Research, University of Arizona, Tucson, Arizona, U.S.A.

6 <sup>3</sup>NOAA/Pacific Marine Environmental Laboratory, Seattle, Washington, 98115 U.S.A.

7 <sup>4</sup>Cooperative Institute for Marine Resources Studies, Oregon State University, Newport, Oregon, 97366 U.S.A.

8 *Correspondence to:* Robert P. Dziak (Robert.p.dziak@noaa.gov)

9 **Abstract.** We present a spatially focused investigation of the disturbance history of an old-growth Douglass fir stand in South  
10 Beach, Oregon for possible growth effects due to tsunami inundation caused by the A.D. 1700 Cascadia subduction zone  
11 earthquake. A high-resolution model of the 1700 tsunami run-up heights at South Beach, assuming an “L” sized earthquake,  
12 is also presented to better estimate the inundation levels several kilometers inland at the old-growth site. This tsunami model  
13 indicates the South Beach fir stand would have been subjected to local inundation depths from 0-10 m. Growth chronologies  
14 collected from the fir stand shows several trees experienced significant growth reductions before, during and several years  
15 after 1700, consistent with the tsunami inundation estimates. The +/- 1-3 year timing of the South Beach disturbances are also  
16 consistent with disturbances previously observed at a Washington state coastal forest ~220 km to the north. Additional  
17 comparison of the South Beach chronologies with regional chronologies across Oregon indicates the South Beach stand growth  
18 was significantly and unusually lower in 1700. Moreover, the 1700 South Beach growth reductions were not the largest over  
19 the 110-year tree chronology at this location. with other disturbances likely caused by other climate drivers (e.g. drought or  
20 windstorms). Our study represents a first step in using tree growth history to ground-truth tsunami inundation models by  
21 providing site specific physical evidence.

22 .

## 23 1. Introduction

24 Recent catastrophic tsunami inundation events along the Sumatra and Japanese coasts have shown tsunamis can have  
25 a devastating effect on coastal forests and overall coastal geomorphology [Kathiresan and Rajendran, 2005; Udo et  
26 al., 2012; Lopez Caceres et al., 2018]. In addition to the tsunami, ground motion caused by the megathrust earthquake  
27 can cause significant forest disturbance by toppling trees, damaging root systems, severing limbs and crowns,  
28 inducing damaging landslides, or altering the hydrology of a stand, among other potential effects [e.g. Sheppard and  
29 Jacoby, 1989]. These disturbances appear in the tree-ring record of surviving trees as sudden suppression events  
30 (when there is damage), or growth events in the case of reduced competition from adjacent damaged trees.



31  
32 Here we present a spatially focused investigation of the disturbance history of an old-growth forest in South Beach,  
33 Oregon (**Figure 1**). We also present a new, high resolution model of the 1700 tsunami run-up heights at South Beach  
34 to better estimate the inundation levels at the site of the old-growth forest. Our goal is to use tree-growth to ground-  
35 truth the tsunami impacts and inundation levels as well as for insights into the degree of shaking caused by the 1700  
36 magnitude 9.0 Cascadia Subduction Zone earthquake [Satake et al., 2003; Witter et al., 2011].

37  
38 Interestingly, direct evidence of seismic shaking (liquefaction, landslides, etc) from the 1700 megathrust earthquake  
39 is relatively rare along the Oregon coast. This is thought to be due to the high rainfall and water erosion rates in the  
40 Pacific Northwest which removes liquefaction evidence in coastal estuaries, and makes landslides in the coast range  
41 difficult to identify [Yeats, 2004; LaHusen et al., 2020]. Models of shaking and ground motion along the Oregon  
42 coast during the 1700 Cascadia earthquake indicate it should have been violent and widespread [WDNR, 2012], and  
43 it seems plausible that evidence of this shaking might be recorded in the ring widths of trees along the coast.

44  
45 Very little tree-ring work has been conducted along the Oregon coast; the vast majority of tree-ring research in the  
46 Pacific Northwest has entailed climate reconstructions from high-elevation sites in the Cascade Mountains and  
47 Olympic Peninsula where competitive effects are low. We sampled a mesic old-growth forest near the Pacific coast  
48 where competitive effects are high. Significant disturbances from the 1700 earthquake and tsunami should  
49 substantially alter radial growth patterns as some trees are damaged or killed and resources are redistributed to  
50 survivors. Alternatively, the tsunami may cause physical damage to trees resulting in growth reductions. The goal of  
51 this study is to investigate whether these disturbances are observable in the few remaining old-growth forests along  
52 the coast of Oregon. Thus we chose a site where good inundation models exist, and there is significant public concern  
53 about tsunami impacts because of the presence of a large population and municipal infrastructure.

## 54 55 **2.0 Evidence for Megathrust Earthquakes and Tsunamis**

56  
57 On 26 January at 9:00PM in the year 1700 A.D., a large earthquake occurred on the Cascadia Subduction Zone, the  
58 boundary between the Pacific and North American plates along the coasts of California, Oregon, Washington, and  
59 British Columbia [Satake et al., 2003]. The earthquake created a tsunami with 10-12 m run-up heights that struck the  
60 Pacific Northwest and propagated across the Pacific to Japan [Atwater, 1992; Satake, et al, 2003; Goldfinger et al.,  
61 2003]. The 1700 earthquake is estimated to have most likely been a moment magnitude ( $M_w$ ) 9.0, with between 13-  
62 21 m of coseismic slip on an offshore fault 1100 km long [Satake et al., 2003; Witter et al., 2011]. The 1700 earthquake  
63 was preceded by an earthquake in 960 A.D. (740 yr interval) and another in 750 A.D. (210 yr interval), with three  
64 additional subduction events before these that comprise a recent cluster of 6 megathrust events over the past 1500 yrs



65 [Atwater et al., 2003]. During the 1700 Cascadia earthquake, ground motion and peak ground acceleration (PGA),  
66 are modeled to have ranged from ~0.5-1.2 g along the Oregon coast [WDNR, 2012]. Thus ground motion shaking  
67 during the 1700 earthquake should have been violent and widespread.

68  
69 The exact timing of the earthquake was estimated by calculating the travel time for an unexplained tsunami that struck  
70 Japan on 26 January 1700 [Satake et al., 2003; Atwater, 2006]. Radiocarbon dating was used to show the earthquake  
71 occurred in 1700, where the radiocarbon dates were derived from the remnants of many trees drowned by coincident  
72 subsidence, and surviving trees recorded the earthquake's date by anomalous changes in ring width or anatomy of  
73 their annual rings [Atwater and Yamaguchi, 1991; Jacoby et al., 1997]. As a result of subsidence, some coastal forests  
74 dropped below sea level and were flooded. Boles and root masses of these trees still remain and can be found from  
75 northern Oregon to southern Washington. Aligning tree-ring growth patterns of the living trees with those of the  
76 flooded, dead trees consistently showed that the last year of growth was 1699, indicating the earthquake occurred  
77 between October 1699 and April 1700 [Yamaguchi et al., 1997]. This tree-ring and dating evidence for coastal  
78 disturbance is indeed compelling, however the evidence was derived from trees along just 100 km of coastal southern  
79 Washington-northern Oregon, or ~5% of the coastline expected to be affected by a Cascadia megathrust earthquake.

80  
81 Additionally, a coastal-wide inventory of liquefaction features associated with the 1700 earthquake found no features  
82 along the Oregon coast, despite numerous exposures of clean sand deposits that must be susceptible to liquefaction,  
83 even at low levels of seismic shaking [Obermeier and Dickenson, 2000]. The locations for these field studies in  
84 Oregon were also sites where evidence for great Holocene subduction earthquakes (in the form of crustal subsidence)  
85 have been identified [Nelson et al., 1995]. The only liquefaction features identified to date (and thus direct evidence  
86 of seismic shaking) were found along the Columbia River 35-50 km east of the coast, and these indicate moderate  
87 shaking intensity of 0.2-0.35 g [Obermeier and Dickenson, 2000].

### 88 89 **3.0 Model of A.D. 1700 Tsunami**

90  
91 As a first step in estimating tree disturbance in South Beach, we produced a model of tsunami inundation level and  
92 expected flow speed for the 1700 earthquake based on estimates of size, location, displacement and coastal subsidence  
93 [Figures 2a,b,c; Witter et al, 2011]. Thus the modeled run-up height of the 1700 tsunami can be used as a basis to  
94 investigate possible impacts along the coast and estuaries of South Beach.

95 **Figures 2a,b** show the model results of tsunami inundation level and flow speed for South Beach assuming the “L”  
96 or large sized earthquake (Mw 9.0) for the A.D. 1700 event [Wei, 2017]. The L model assumes a finite-fault source  
97 with maximum vertical coseismic displacement of 15.2 m and subsidence of ~1.03 m at South Beach [Figure 2c;  
98 Witter et al., 2011]. The Witter et al. (2011) coseismic subsidence estimate differs slightly from the Satake et al (2003)



99 because it is based on coseismic slip from turbidite records [Goldfinger, 2011], and includes a rupture model with  
100 slip partition into a splay fault in the accretionary wedge. The earthquake source duration was not taken into account  
101 in the model.

102  
103 Two models were used to compute the tsunami inundation levels and flow speed [Wei, 2017] based on four-level  
104 telescoped model grids at the spatial resolutions of 1 arc min (~ 1.8 km), 12 arc sec (~ 360 m), 2 arc sec (~ 60 m),  
105 and 1/6 arc sec (~ 5 m). The MOST model [Titov and Gonzalez, 1997] is based on the shallow-water wave equations  
106 and uses the estimates of coseismic slip to account for deep-water wave propagation. The MOST model then provides  
107 the boundary conditions computed from the level-1 grid (**Figure 2a**) for a Boussinesq model [Zhou et al., 2011],  
108 which takes into account frequency dispersion when computing the nearshore wave-propagation field and onshore  
109 tsunami inundation in level-2, 3, and 4 grids (**Figure 2b** shows the coverage of level-4 grid). The digital-elevation  
110 and bathymetric grid of Newport-South Beach in level 4 used in the tsunami inundation models has a spatial resolution  
111 of 1/6 arc sec (~5 m). It is derived from the Digital Elevation Model provided by the Oregon Department of Geology  
112 and Mineral Industries (DOGAMI). This dataset contains lidar data based on DOGAMI Lidar Data Quadrangles for  
113 Toledo South, Newport North, and Newport South. The horizontal datum is WGS 84. The vertical datum is NAVD  
114 1988, and it is then converted to Mean Higher High Water (MHHW) level, which is the vertical datum in our tsunami  
115 inundation models. MHHW is 2.317 m above the NAVD 1988, and 1.185 m above Mean Sea Level (MSL) at Newport  
116 according to the datum information at the National Ocean Service (NOS) tide gauge at South Beach. Typically when  
117 performing hazard assessments, Mean High Water (MHW) or MHHW is assumed over the entire duration of tsunami  
118 [Wei, 2017], and using MHHW as the vertical datum usually gives a more conservative estimate of the tsunami  
119 impact. In the present study, we prefer to use MHHW, instead of the actual tidal level, as our model reference level  
120 due to: 1) the uncertainty of the time of the event, which is based on estimates from Japanese records (Satake et al.  
121 1996), and could vary over a window of 1-2 hours; 2) the uncertainty of the earthquake/tsunami source; and 3) the  
122 uncertainty in the amount of sea level change, which is > 0.5 m over the past 300 years based on a rate of 1.77 mm  
123 annual increase. The impact of these uncertainties on the model could overshadow the difference between MHHW  
124 and the actual tidal level, and adds an additional level of uncertainty to the model results. A Manning's coefficient of  
125 friction of 0.03 is uniformly applied for both the land and ocean components of the tsunami propagation model. To  
126 more realistically estimate the tsunami impact produced by the 1700 event, we removed the two jetties at the entrance  
127 of Yaquina Bay from the model DEMs, which leads to greater tsunami inundation levels and impact at South Beach.  
128 The tsunami model results discussed hereafter are based on the revised DEMs without the jetties.

129  
130 The tsunami inundation model presented here indicates the "L" earthquake, with the co-seismic subsidence taken into  
131 account, would produce a tsunami that could inundate South Beach to tsunami water levels up to 17 m (**Figure 2a**),  
132 and inundation depths up to 16 m (**Figure 3a,b**). The height of the water level at the western section of Mike Miller



133 Park is generally between 12-15 m, and reduces to between 9-12 m on the eastern side. It is important to note that  
134 “tsunami water level” is a term used to describe the elevation reached by seawater measured relative to a stated datum  
135 (MHHW herein). Whereas “inundation depth” refers to the local water depth, or height of the tsunami above the  
136 ground after taking into account the co-seismic subsidence at a specific location, as shown in Figure 2c. However,  
137 there is significant variation in the topography of South Beach, and several areas are predicted to experience a range  
138 of inundation depths much less than the 16 m maximum. For example, the model shows the amount of inundation  
139 decreases eastward of the beach, and the location of the old-growth Douglas Fir stand at Mike Miller State Park in  
140 South Beach may be subjected to a range of inundation depth from negligible to as much as 10 m (**Figure 3b**).  
141 Moreover, the South Beach stand would likely have been subjected to flow velocities between 2-10 m s<sup>-1</sup> (**Figure**  
142 **2B**). These velocities are lower than most of the westward portions of the South Beach Peninsula because the stand  
143 is located on topography that can be up to 10 m higher elevation than most of the westward terrain. Nevertheless, it  
144 would seem these tsunami current velocities would be high enough to cause significant damage to the South Beach  
145 trees, through the large mass and momentum of this volume of sea water, that would be observable in the tree growth.  
146

147 Lastly, it is worth noting that the “L” earthquake tsunami model presented here also involves the activation of splay  
148 faults in the overriding plate above the subduction zone. Motion on these splay faults introduce a larger co-seismic  
149 subsidence along the coastline, and therefore represent a more extreme inundation scenario for the A.D. 1700 event  
150 than previous models. Based on the turbidites records reported by Goldfinger et al. (2011), the “L” and larger  
151 earthquake scenarios occurred four times in the past 10,000 years, and thus is referred as a 2,500-year event, although  
152 the general earthquake size class and associated time interval for an “L” event is estimated to be 800 years by Witter  
153 et al. (2011).

#### 154 155 **4.0 Impacts of Earthquakes and Tsunamis Inundation on Tree Growth**

##### 156 157 *4.1 Earthquake induced ring growth disturbance*

158 Although there is evidence for only moderate levels of ground shaking in coastal Oregon and Washington following  
159 the 1700 earthquake [Obermeier and Dickenson, 2000], ground motion during large earthquakes has been shown to  
160 cause significant forest disturbance in other earthquake prone regions. As previously mentioned, these earthquake-  
161 induced disturbances are caused by felling or damaging trees, inducing local landslides, or altering the stand’s water  
162 access [Jacoby et al, 1997]. Trees that survive these disturbances can have a tree-ring record that shows both sudden  
163 growth suppression events, or even sudden positive growth events because of possible reduced competition from  
164 nearby damaged trees. Moreover, pulses in tree recruitment may follow a large earthquake as young trees colonize  
165 gaps left by damaged over-story individuals [Jacoby et al., 1997].  
166



167 Trees can respond both directly and indirectly to the effects of large earthquakes. Indirect responses can occur due to  
168 coseismic environmental changes. For example, Fuller (1912) noted trees died from flooding during the 1811-1812  
169 New Madrid earthquakes. Wallace and LaMarche (1979) found coast redwoods (*Sequoia sempervirens*) and  
170 Douglas-firs (*Pseudotsuga menziesii*) tilted by the 1906 San Andreas Fault earthquake had reaction wood growth  
171 starting in 1907. Meisling and Sieh (1980) reported the January 1857 Ft. Tejon earthquake caused conifers to lose  
172 their crowns, which reduced ring widths that took many years to return to pre-earthquake growth rates. Jacoby and  
173 Ulan (1983) showed the September 1899 Alaska earthquake caused near shore Sitka spruces (*Picea sitchensis*) to  
174 increase growth because coseismic uplift moved the shoreline, resulting in less exposure to wind, salt spray, and root-  
175 zone erosion. As for direct responses to earthquake impacts, Jacoby et al., (1988) analyzed conifer tree-ring samples  
176 near the epicenter of the 1812 San Juan Capistrano earthquake. A total of nine on-fault trees showed drastic growth  
177 reductions in 1813, requiring decades to return to pre-disturbance growth rates. Similarly, Shephard and Jacoby  
178 (1989) showed that the 1964 Alaskan earthquake, which caused ~4 m of coseismic uplift, initially induced growth  
179 reduction in Sitka Spruces, but the trees eventually responded with wide reaction wood rings in the following years  
180 to regain upright positions.

181

#### 182 4.2 Tsunami induced tree-ring growth disturbance

183 Just as trees located near epicenters of large earthquakes can be disturbed and show growth changes from intense  
184 shaking and ground displacement, inundation of a coastal forest by a large tsunami should also have a significant  
185 impact. Catastrophic tsunami inundation events along the Sumatra and Japanese coasts showed tsunamis have a  
186 devastating effect on coastal forests, damaging trees and severely eroded and alter the beach and estuary  
187 geomorphology [e.g. Kathiresan and Rajendran, 2005; Udo et al., 2012; Lopez Caceres et al., 2018]. It is expected  
188 that inundation by a tsunami would cause significant ring-growth reduction due to physical impact from the wave,  
189 prolonged exposure to salt-water, and from tsunami debris that would also physically impact the tree.

190

191 In the U.S. Pacific Northwest, when the A.D. 1700 co-seismic tree-ring growth disturbance is considered, it is largely  
192 of trees killed by inundation attributed to co-seismic subsidence [e.g. Atwater and Yamaguchi, 1991]. However,  
193 Jacoby et al., [1997] were able to find trees that pre-dated the 1700 Cascadia earthquake and survived subsidence and  
194 inundation, which is analogous to the tree-ring growth scenario we observed in South Beach, Oregon.

195

196 Jacoby et al. [1997] collected cores from 33 living Sitka spruce trees that were established earlier than 1700 (i.e. at  
197 least 300 years old) that stand along the western Columbia River between Washington and Oregon (~220 km north  
198 of South Beach). While 15 of these trees show some evidence of disturbance at 1700, 5 trees showed no disturbance  
199 and the remaining 14 could be in either category. There were both unusual decreases and increases in ring-width in  
200 disturbed trees. Disturbed trees also showed water-logging and increasing numbers of traumatic resin canals at 1700



201 (sap-conducting tubes formed by altered cells), but only 2 show reaction wood formation in response to co-seismic  
202 tilting or flooding. All trees also display a wide range in the years that ring-width changes begin, with clear decline  
203 in growth occurring as early as 1698 and as late as 1702 up to 1706.

204  
205 Thus the exact timing of tree-ring disturbances due to an earthquake and the resulting ground motion, coastal land  
206 subsidence and tsunami inundation can vary within a few years around the event date. This is because tree growth  
207 can be affected by several climatological/meteorological factors, including droughts, cold/heat stress, fires, and  
208 windstorms and even insect infestations. However, comparison of coastal growth rings with other regional sites can  
209 be used to control for these climate/weather disturbance impacts. Thus, despite this temporal variability, Jacoby et al  
210 (1997) conclude the subduction earthquake/subsidence event occurred between the growing seasons of 1699 and  
211 1700. Thus it seems likely a combination of the effects from earthquake ground motion, coastal land subsidence, and  
212 rapid inundation by several meters of fast moving sea water can be observed in the variation of ring growth  
213 chronologies from trees within the impact zone.

214

## 215 **5.0 Tree Ring Growth Chronologies from South Beach, Oregon**

216

217 In an attempt to further quantify the widespread effects of the A.D. 1700 earthquake, we obtained tree-ring records  
218 from a stand of old-growth Douglas fir trees (*Pseudotsuga menziesii*) whose ages pre-date 1700 (**Figure 4a,b**). The  
219 stand is located in an Oregon State Park in South Beach, Oregon, roughly 600 m east of Highway 101 (**Figure 3a,b**).  
220 Old growth trees of 300+ years of age are rare along the Oregon coast, thus this stand of trees within the inundation  
221 zone presented a unique opportunity to search for direct physical evidence of the impact of a Cascadia Subduction  
222 zone earthquake and tsunami inundation in a populated area where tsunami models indicate significant inundation  
223 levels and run-up heights.

224

225 To ground-truth the model of the A.D. 1700 tsunami, we collected tree cores at breast height from 37 dominant or  
226 codominant old-growth trees at the South Beach site using a 32" increment borer. Two cores were collected from  
227 each tree, after which cores were mounted, sanded with increasingly fine lapping film, and cross-dated (Phipps 1985).  
228 Each core was then measured using a Velmex TA Tree-Ring Measuring device to the nearest 0.001mm (Velmex, Inc.  
229 Bloomfield, NY). Cross-dating was then statistically verified using the program COFECHA [Holmes 1983]. A master  
230 growth-increment chronology was then developed by detrending each measurement time series using a negative  
231 exponential or regression functions to retain as much low-frequency variability as possible as well as a second  
232 chronology developed using 50-year 50% frequency-cutoff cubic spline to highlight interdecadal to interannual  
233 growth variability. All chronology construction was performed using the program ARSTAN Cook and Krusic 2005].  
234 **Figure 3a,b** shows the location of the Douglas Fir trees sampled for this study in relation to the modeled tsunami



235 run-up heights for South Beach. Of all the trees sampled, a total of twelve cores from eight trees pre-dated 1700  
236 **(Figure 4b)**.

237

238 As noted, the tsunami inundation model presented here (**Figure 2a,b**) indicates the “L” earthquake would produce a  
239 tsunami that could inundate the lowlands of South Beach to inundation depths up to 18 m. However, the Douglas fir  
240 old-growth stand that is the subject of this study lies on, and along the western edge, of two parallel north-south  
241 striking topographic highs (likely paleo-dune ridge lines). The tsunami model presented here indicates that while  
242 many of the trees in this area may have experienced as much as ~10 m of inundation depth, several trees are also on  
243 high ground and may have experienced much less, or even zero, inundation.

244

245 Tree-ring data detrended using negative exponential functions did not reveal major stand-wide releases or  
246 suppressions around 1700 (data not shown) nor did data detrended using the 50-year spline functions. Detailed  
247 examination of the growth-ring samples indicates that although individual cores have below-average growth, and one  
248 experiences what could be interpreted as a post-1700 growth release, variability around 1700 is not necessarily  
249 exceptional in the longer-term context of the ~310 year history of the dataset (**Figure 4a,b**). Indeed, there are at least  
250 5 other growth reductions in the record that are the same magnitude or larger than the disturbance at A.D. 1700. Most  
251 notably, there are large suppressions observed beginning around 1691 and again in 1739 and 1745 (**Figure 4a**). The  
252 1739 reduction has been observed in other old-growth stand chronologies throughout Cascadia and may be due to a  
253 significant climatological event such as a drought [Carroll et al. 2005, 2014].

254

### 255 *5.1 Control Sites in Western Oregon Cascades and Coast Range*

256

257 To better detect unusual growth anomalies around 1700, we compared the South Beach Douglas fir tree-ring data to  
258 two other Douglas-fir data sets from the Oregon Coast Range and western Cascade Mountains, which would have  
259 experienced similar climate conditions but not tsunami inundation. The first of these was an old-growth stand on  
260 Marys Peak (~46 km east of South Beach) in the central Coast Range and Browder Creek located ~160 km east in the  
261 western Cascade Mountains [Black et al. 2015; **Figure 5a,b**]. The other was a chronology generated from dead-  
262 sampled trees in lakes in the western and central Oregon Coast Range. These lakes had formed when landslides  
263 impounded streams, and the preserved drowned trees were then used to establish the date of lake formation, and thus  
264 the landslide event [Struble et al. 2020]. Eight lakes had a combined number of 15 trees (and 31 sets of measurements)  
265 that pre-dated 1700 and were used to generate a second “control” chronology. As with Mike Miller trees, all  
266 measurement time series in the control datasets were detrended with 50-year splines.

267





268 When compared to the control sites, South Beach tree growth is significantly lower than the lakes or Marys Peak in  
269 1700 (t-test of  $p < 0.001$ ). Moreover, the lakes trees and Marys Peak trees do not significantly differ in growth in 1700,  
270 suggesting the South Beach Douglas fir growth is unusually low across sites with similar climatic histories and  
271 sensitivities.

## 272 **6.0 Discussion**

273  
274  
275 Analysis of tree-ring data presented here indicates there is a reduction in Douglas-fir tree growth at a site associated  
276 with the 1700 Cascadia Subduction Zone earthquake and tsunami in South Beach Oregon relative to other inland,  
277 sites in the Oregon coast range. The growth reduction is not outside the range of variability, as illustrated by other  
278 much more severe suppressions over the 310 year South Beach chronology (**Figure 5a,b**). However, there is at least  
279 a subtle growth reduction that deviates from other nearby locations.

280  
281 The tsunami inundation model presented here, which assumes the “L” or large sized earthquake (Mw 9.0) for the  
282 1700 event [Wei, 2017] shows the resulting tsunami would have inundated the South Beach Douglas-fir stand. The  
283 growth reduction in Douglas-fir at South Beach, while not absolute conclusive evidence, is at least consistent with  
284 such an event and with both the magnitude and multi-year time period of growth reductions observed by Jacoby et al  
285 (1997) along the Columbia River ~220 km to the north.

286  
287 Although tree rings and various geologic lines of evidence have been useful in establishing the date of the last  
288 Cascadia earthquake, there is still some question as to the degree of peak ground motion associated with the event.  
289 As previously discussed, a coastal-wide inventory of liquefaction features associated with the 1700 CSZ event  
290 indicate only moderate levels of ground shaking in coastal Oregon and Washington [Obermeier and Dickenson,  
291 2000]. Mapping seismically induced landslides in the Oregon coast range is potentially another means to assess  
292 levels and distribution of seismic shaking impacts from the 1700 CSZ event, given large-magnitude earthquakes in  
293 mountainous regions around the world typically trigger thousands of landslides, and slope failures constitute a  
294 significant proportion of the damage associated with these events [Stuble et al. 2020]. Recent studies have  
295 demonstrated the utility of dendrochronology to date the ages of landslides in these settings [Stuble et al., 2020].  
296 However, despite the Oregon coast range exhibiting thousands of landslides, none have been conclusively associated  
297 with the 1700 subduction earthquake, and despite proximity to the megathrust rupture, most deep-seated landslides in  
298 the Oregon Coast Range were triggered by rainfall [LaHusan et al., 2020]. Thus a continued search for physical  
299 evidence of tsunami inundation, earthquake shaking, and co-seismic landslides is needed to refine expectations of the  
300 inundation as well as intensity and distribution of ground shaking during future Cascadia megathrust earthquakes.  
301



## 302 **7.0 Summary**

303 We presented a series of tree-ring data from an old-growth Douglas-fir forest in South Beach, Oregon that shows  
304 significant growth disturbance at the time of the A.D. 1700 Cascadia subduction zone earthquake. In addition, we  
305 presented a new, high resolution model of the 1700 tsunami inundation at South Beach old-growth site. Due to  
306 significant variation in the South Beach topography, several areas are predicted to experience water levels up to 17  
307 m and a range of inundation depths up to 16 m, however the location of the old-growth stand may be subjected to a  
308 range of inundation depths from 0-10 m. To better detect tree growth anomalies near AD 1700, we also compared the  
309 South Beach Douglas-fir tree-ring data to two other Douglas-fir data sets from the Oregon Coast Range and western  
310 Cascade Mountains, which would have experienced similar climate conditions but not tsunami inundation. When  
311 compared to these control sites, South Beach tree growth is significantly lower in 1700, and reaffirms that the South  
312 Beach Douglas-fir growth is unusually low for the region. Thus the timing of the observed growth reductions in the  
313 South Beach Douglas-fir stand is consistent with these disturbances being associated with the A.D. 1700 Cascadia  
314 megathrust earthquake and the resulting tsunami, subsidence and ground motion. Overall, we think our study further  
315 supports the view that tree-ring data is a promising tool for providing insights on the spatial distribution of co-seismic  
316 impacts from megathrust earthquakes, as well as potential ground-truth information for tsunami inundation models.

317

## 318 **8. Sample Availability**

319 Upon acceptance of the manuscript, the Mike Miller, Cape Perpetua, and Marys Peak tree-ring data used in this  
320 study will be contributed to the NOAA National Centers for Environmental Information International Tree-Ring  
321 Databank, <https://www.ncdc.noaa.gov/data-access/paleoclimatology-data/datasets/tree-ring>

## 322 **9. Code Availability**

323 The tsunami model can be made available with a request to [oar.pmel.tsunami-webmaster@noaa.gov](mailto:oar.pmel.tsunami-webmaster@noaa.gov) followed by a  
324 model software training course provided by the NOAA Center for Tsunami Research

## 325 **10. Author Contribution**

326 RD prepared the manuscript with contributions from all co-authors. BB and RD collected the tree-ring samples,  
327 performed growth disturbance analysis, and wrote the manuscript. YW developed the tsunami model code and  
328 performed the simulations, and wrote tsunami section of manuscript. SM drafted initial maps used in manuscript.

## 329 **11. Competing Interests**

330 The authors declare that they have no conflict of interest.

## 331 **12. Acknowledgements**

332

333 The authors wish to thank the editor and two reviewers. The research in this paper was sponsored by the  
334 NOAA/Pacific Marine Environmental Laboratory, PMEL paper contribution number 5184. Yong Wei's work is  
335 funded by the Joint Institute for the Study of the Atmosphere and Ocean (JISAO) under NOAA Cooperative  
336 Agreement NA15OAR4320063, Contribution No. 2020-1084. All data is available from the authors upon request,  
337 without undue reservation, to any qualified researcher .



## 338 References

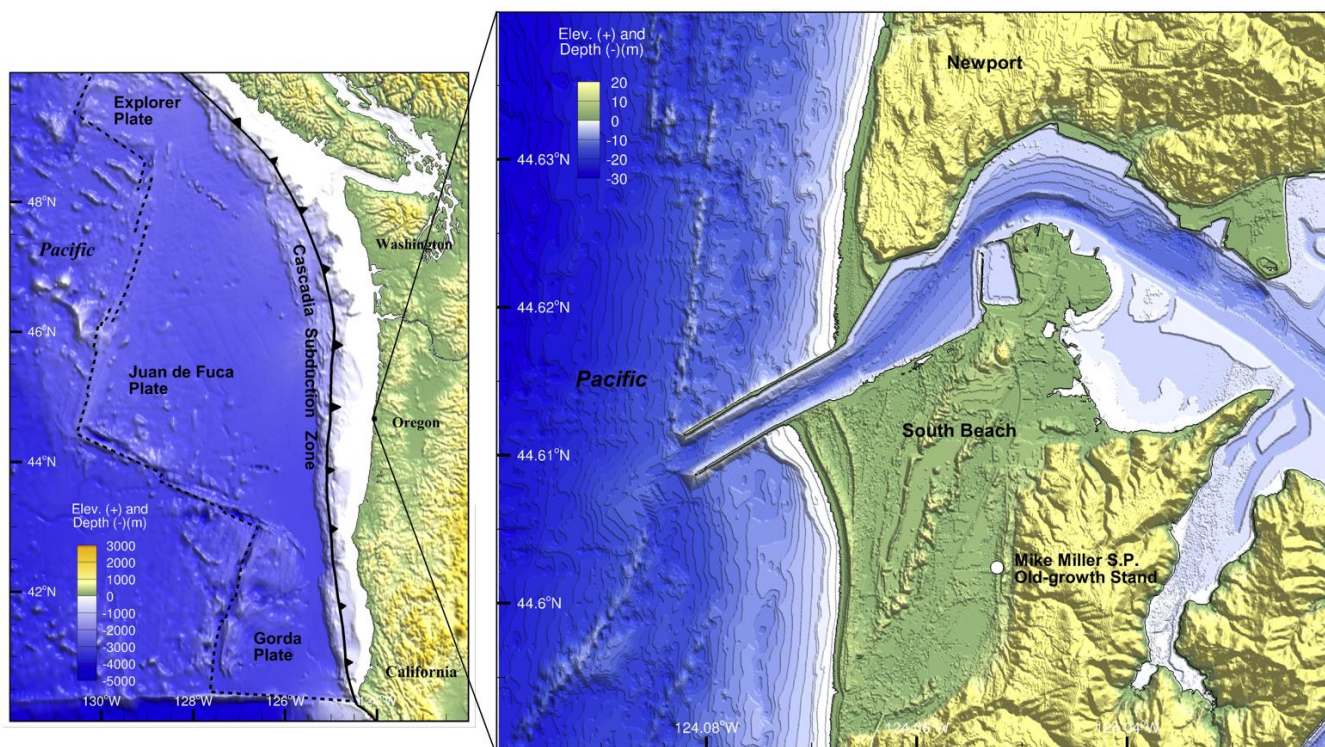
- 339 Atwater, B.F. and D.K. Yamaguchi (1991). Sudden, probably coseismic submergence of Holocene trees and grass in coastal  
340 Washington State. *Geology*, 19(7), 706-709.
- 341 Atwater, B. F., (1992). Geologic evidence for earthquakes during the past 2000 years along the Copalis River, southern  
342 coastal Washington. *J. Geophys. Res.*, 97, 1901–1919
- 343 Atwater, B.F., M. P. Tuttle, E.S. Schweig, C.M. Rubin, D.K. Yamaguchi, and E. Hemphill-Haley (2003). Earthquake  
344 recurrence inferred from paleoseismology. *Developments in Quaternary Science*, 1, 331-350.
- 345 Atwater, B., M.R. Satoko, K. Satake, T. Yoshinobu, U. Kazue, D.K. Yamaguchi (2006). The orphan tsunami of 1700-  
346 Japanese clues t a parent earthquake in the North America. *U.S. Geol. Survey Professional Paper* 1707, 14p.
- 347 Black, B.A., Dunham, J.B., Blundon, B.W., Brim-Box, J., Tepley, A.J., 2015. Long-term growth-increment chronologies  
348 reveal diverse influences of climate forcing on freshwater and forest biota in the Pacific Northwest. *Global Change*  
349 *Biol.* 21, 594-604.
- 350 Carroll, A.L., and Jules, E.S. (2005). Climatic assessment of a 580-year *Chamaecyparis Lawsoniana* (Port Orford cedar)  
351 tree-ring chronology in the Siskiyou mountains, USA. *Madrono* 52, 114-122, 119.
- 352 Carroll, A.L., Sillett, S.C., Kramer, R.D. (2014). Millennium-Scale Crossdating and Inter-Annual Climate Sensitivities of  
353 Standing California Redwoods. *PLOS ONE* 9, e102545. doi:10.1371/journal.pone.0102545.
- 354 Cook, E.R., Krusic, P.J. (2005). ARSTAN v. 41d: A tree-ring standardization program based on detrending and  
355 autoregressive time series modeling, with interactive graphics. Tree-Ring Laboratory, Lamont-Doherty Earth  
356 Observatory of Columbia University, Palisades, New York, USA.
- 357 Fuller, M.L. (1912). The New Madrid earthquake, *U.S. Geological Survey Bulletin*, 494, 119 pp.
- 358 Goldfinger, C., C.H. Nelson, J.E. Johnson (2003). Holocene earthquake records from the Cascadia Subduction Zone and  
359 northern San Andreas Fault based on precise dating of offshore turbidites. *Annu. Rev. Earth Planet. Sci.*, 31, 555-  
360 577, doi:10.1146/annurev.earth.31.100901.141246.
- 361 Goldfinger, C. (2011). Submarine paleoseismology based on turbidite records. *Ann Rev. Mar. Sci.* v:3, 35-66.
- 362 Holmes, R.L. (1983). Computer-assisted quality control in tree-ring dating and measurement. *Tree-Ring Bull.* 43, 69-78.
- 363 Jacoby, G.C. and L.D. Ulan (1983). Tree ring indications of uplift at Icy Cape, Alaska, related to 1899 earthquakes. *J.*  
364 *Geophys. Res.*, v:88, B11, <https://doi.org/10.1029/JB088iB11p09305>
- 365 Jacoby, G.C., P.R. Sheppard, and K.E. Sieh (1988). Irregular recurrence of large earthquakes along the San Andreas Fault:  
366 Evidence from Trees. *Science*, 241, 4862, 196-199.
- 367 Jacoby, G.C., D.E. Bunker, B.E. Benson (1997). Tree-ring evidence for an A.D. 1700 Cascadia earthquake in Washington  
368 and northern Oregon. *Geology*, v:25, 11, 999-1002.
- 369 Kathiresan, K, and N. Rajendran (2005). Coastal mangrove forest mitigated tsunami. *Estuarine, Coastal and Shelf Science*,  
370 65, 3, 601-606.
- 371 LaHusen, S. R., A. R. Duvall1, A. M. Booth, A. Grant, B. A. Mishkin, D. R. Montgomery, W. Struble, J. J. Roering, J. Wartman  
372 (2020). Rainfall triggers more deep-seated landslides than Cascadia earthquakes in the Oregon Coast Range, USA,  
373 *Sci Advances*, 6 (38), DOI:10.1126/sciadv.aba6790
- 374 Lopez Caceres, M.L., S. Kakano, J.P. Ferrio, M. Hayashi, T. Nakatsuka, T. Yamanaka, Y. Nobori (2018). Evaluation of the  
375 effect of the 2011 tsunami on coastal forests by means of multiple isotopic analyses of tree-rings, *Iso. Env.*  
376 *Health Stud.*, 54:5, 494-507, doi:10.1080/10256016.2018.1495203.
- 377 Meisling, K.E., and K.E. Sieh (1980). Disturbance of trees by the 1857 Fort Tejon earthquake, CA, *J. Geophys. Res.*, 85,  
378 3225-3238.
- 379 Nelson, A. R., B. F. Atwater, P. T. Bobrowsky, L. A. Bradley, J. J. Clague, G. A. Carver, M. K. Darienzo, W. C. Grant, H.  
380 W. Kruger, R. Sparks, T. W. Stafford, and M. Stuiver (1995). Radiocarbon evidence for extensive plate-boundary  
381 rupture about 300 years ago at the Cascadia subduction zone, *Nature* 378, 371–374.
- 382 Obermeier, S.F., and S.E. Dickenson (2000). Liquefaction evidence for the strength of ground motion resulting from Late  
383 Holocene Cascadia Subduction earthquakes, with emphasis on the event of 1700 A.D., *Bull. Seism. Soc. Am.*, 90,  
384 4, 876-896.
- 385 Phipps, R.L. (1985). Collecting, preparing, crossdating, and measuring increment cores. US Geological Survey Water-  
386 Resources Investigations Report 85-4148, 1-47.



- 387 Priest, G.R., R.C. Witter, Y.J. Zhang, K. Wang (2013). Tsunami inundation scenarios for Oregon, Open-file Report 0-13-19,  
388 State of Oregon Department of Geology and Mineral Industries, 14pp.
- 389 Satake, K., K. Shimazaki, Y. Shuji, and K. Ueda (1996), Time and size of a giant earthquake in Cascadia inferred from  
390 Japanese tsunami records of January 1700, *Nature*, 379, 246-249.
- 391 Satake, K., K. Wang, and B. F. Atwater (2003), Fault slip and seismic moment of the 1700 Cascadia earthquake inferred  
392 from Japanese tsunami descriptions, *J. Geophys. Res.*, 108, 2535, doi:[10.1029/2003JB002521](https://doi.org/10.1029/2003JB002521), B11.
- 393 Sheppard, P.R. and G.C. Jacoby (1989). Application of tree-ring analysis to paleoseismology: Two case studies. *Geology*,  
394 17, 226-229.
- 395
- 396 Struble, W.T., Roering, J.J., Black, B.A., Burns, W.J., Calhoun, N., Wetherell, L. (2020). Dendrochronological dating of  
397 landslides in western Oregon: Searching for signals of the Cascadia A.D. 1700 earthquake. *Geol Soc. Am*  
398 *Bulletin*, 132, 1775-1791. doi:10.1130/b35269.
- 399 Titov, V.V. and F.I. Gonzalez (1997). Implementation and testing of the method of splitting tsunami (MOST) model. *NOAA*  
400 *Technical Memorandum ERL PMEL-112*, 11pp.
- 401 Udo, K., D. Sugawara, H. Tanaka, K. Imai, and A Mano (2012). Impact of the 2011 Tohoku earthquake and tsunami on  
402 beach morphology along the northern Sendai coast. 54, doi.org/10.1142/s057856341250009x.
- 403 WDNR (2012). Modeling a magnitude 9.0 earthquake on the Cascadia Subduction Zone off the Pacific Coast,  
404 [http://www.dnr.wa.gov/Publications/ger\\_seismic\\_scenario\\_cascadia.pdf](http://www.dnr.wa.gov/Publications/ger_seismic_scenario_cascadia.pdf)
- 405 Wallace, R.E. and V.C. LaMarche (1979). Trees as indicators of past movements on the San Andreas Fault, *Earthquake*  
406 *Information Bulletin*, 2, 127-131.
- 407 Wei, Y. (2017), Tsunami inundation modeling for the OSU Marine Studies Initiative Building, report submitted to YGH  
408 Architecture, p39.
- 409 Witter, R.C., Y. Zhang, K. Wang, G.R. Priest, C. Goldfinger, L.L. Stimely, J.T. English and P.A. Ferro (2011), Simulating  
410 tsunami inundation at Bandon, Coos County, Oregon, using hypothetical Cascadia and Alaska earthquake scenarios,  
411 Special Paper 43, State of Oregon Department of Geology and Mineral Industries, 57pp.
- 412 Yamaguchi, D.K. (1991). A simple method for cross-dating increment cores from living trees. *Canadian J. of Forest Res.*,  
413 21(3): 414-416, <https://doi.org/10.1139/x91-053>.
- 414 Yamaguchi, D.K., B.F. Atwater, D.E. Bunker, B.E. Benson, M.S. Reid (1997). Tree-ring dating the 1700 Cascadia  
415 earthquake. *Nature*, 922-923, doi:10.1038/40048.
- 416 Yeats, R.S. (2004). Living with earthquakes in the Pacific Northwest, a survivor's guide, second edition: Corvallis, Oregon  
417 State University Press, 400 p.
- 418 Zhou, H., C.W. Moore, Y. Wei, and V.V. Titov (2011). A nested-grid Boussinesq-type approach to modelling dispersive  
419 propagation and runup of landslide-generated tsunamis. *Natural Hazards and Earth System Sciences*, 11, 2677-  
420 2697
- 421



422



423

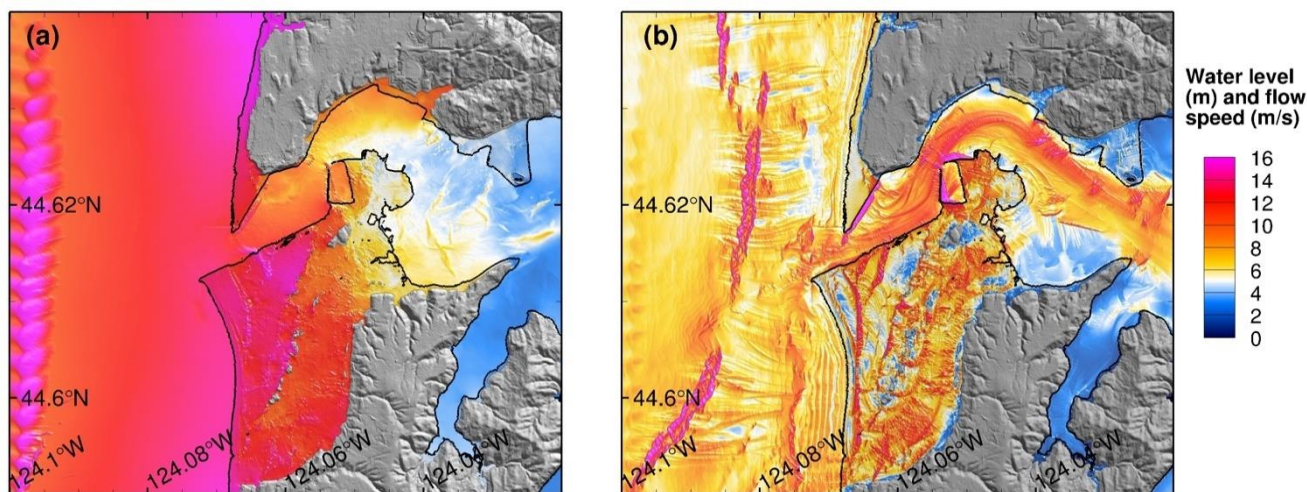
424 **Figure 1:** Map showing location of Newport and South Beach along the central Oregon coast. White dot shows position of  
425 Mike Miller State Park in South Beach, which is location of Douglas fir tree (*Pseudotsuga menziesii*) old growth stand whose  
426 ages extend back past AD 1700. The state park is located ~ 2 km south of the Newport-Yaquina Bay, ~1.2 km east of the  
427 shoreline and ~600 m east of Highway 101. Maps were created using digital elevation data points compiled by National Center  
428 for Environmental Information (<http://ncei.noaa.gov>), and State of Oregon's Department of Geology and Mineral Industries  
429 (<https://www.oregongeology.org/lidar/>).

430

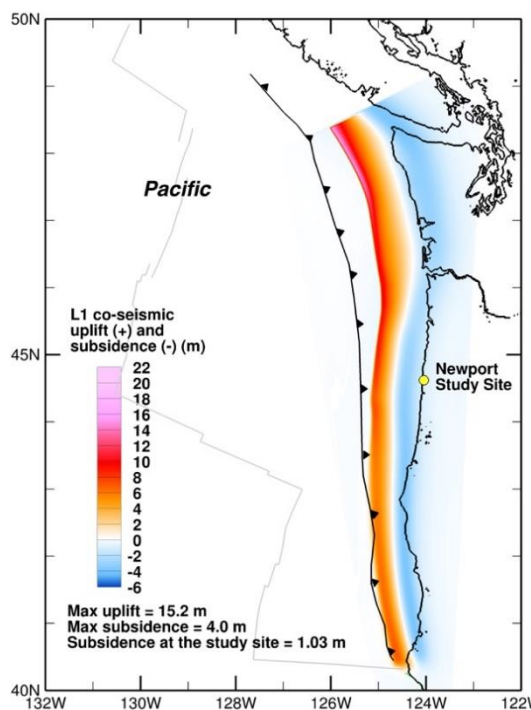
431



432



433



434

435

436

437

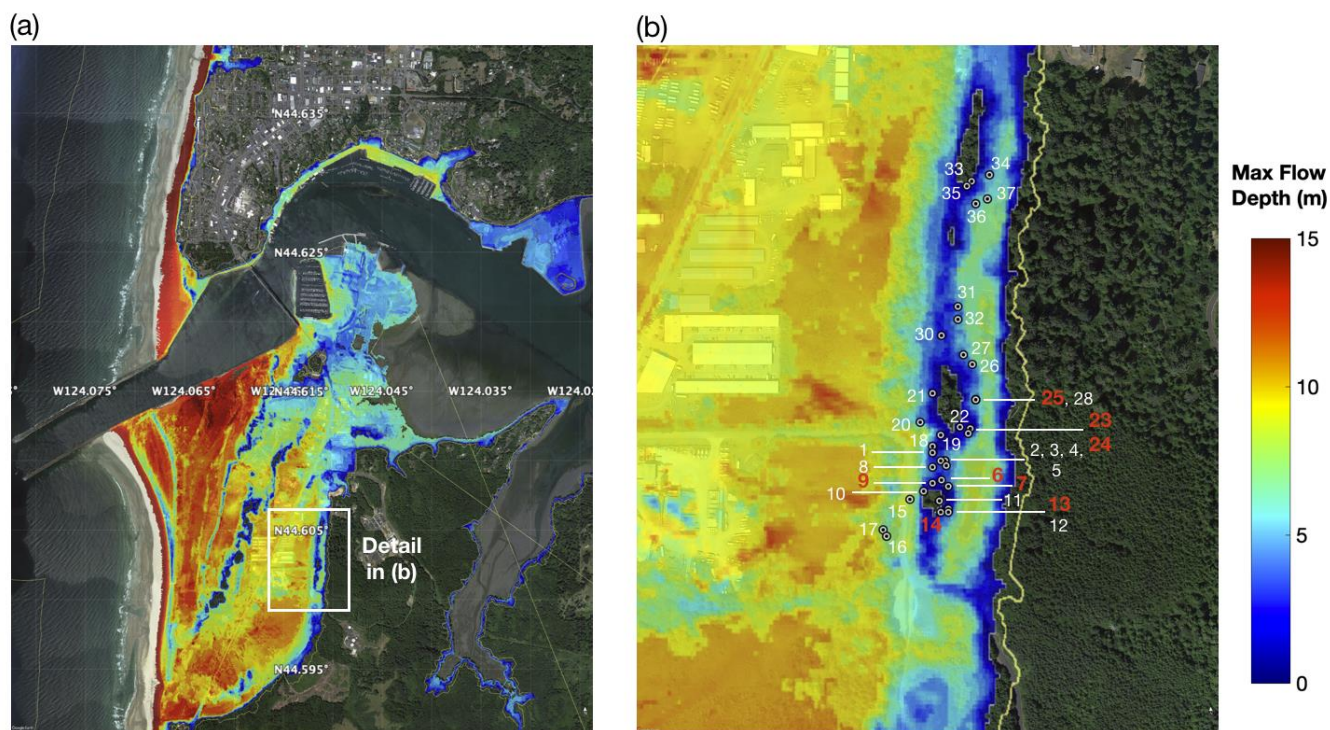
438

439

440

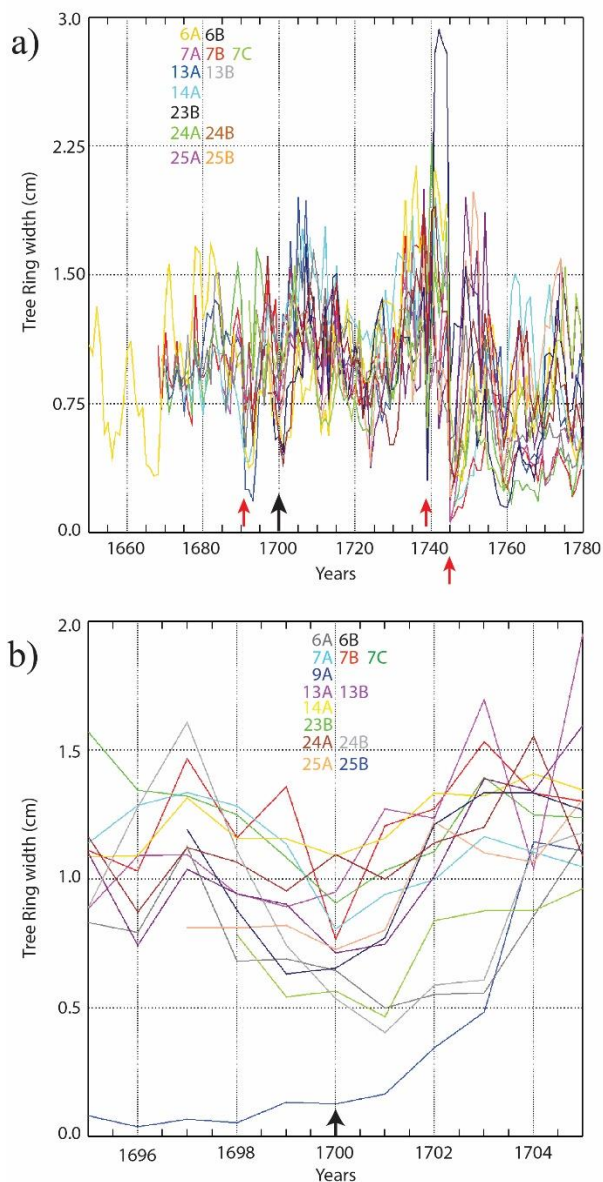
441

**Figure 2:** (a,b) Model of tsunami inundation level and flow speed for South Beach assuming the “L” or large sized earthquake (Mw 9.0) for the A.D. 1700 event [Wei, 2017]. The L model assumes a finite-area fault-source with maximum coseismic displacement of 15.2 m and subsidence of ~1.03 m at South Beach Contour levels are shown. (c) The L model assumes a finite-area fault-source with maximum coseismic displacement of 15.2 m and subsidence of ~1.03 m at South Beach [Witter et al., 2011].



442  
443  
444  
445  
446  
447  
448  
449  
450  
451  
452

**Figure 3:** (a) Model of maximum tsunami inundation depth at South Beach for the “L” sized earthquake A.D. 1700 event; (b) Zoom in view of the tsunami inundation depth at Mike Miller State Park. Gray dotted circles show location of trees used in this study on north side of the Stand. Red numbers are the tree locations whose growth chronologies are shown in **Figure 4a,b**. White numbers shows trees that were cored, but chronologies do not include the years before AD 1700. Colors on map show inundation depth from the model, implying 0-10 m of inundation depth at the Mike Miller Park Douglas fir stand. Green areas are high ground locations that show no inundation. Yellow line shows, for comparison, the model of maximum run-up height for the Mw 9.2 “XXLarge” earthquake scenario [Priest et al., 2013]. Base maps made using © Google Earth 2016.

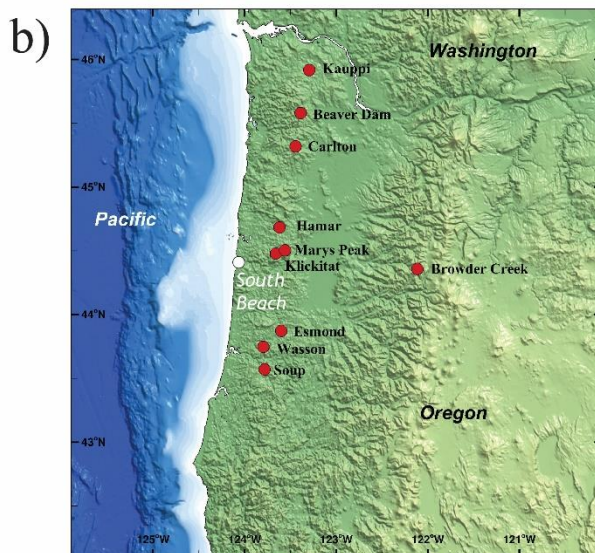
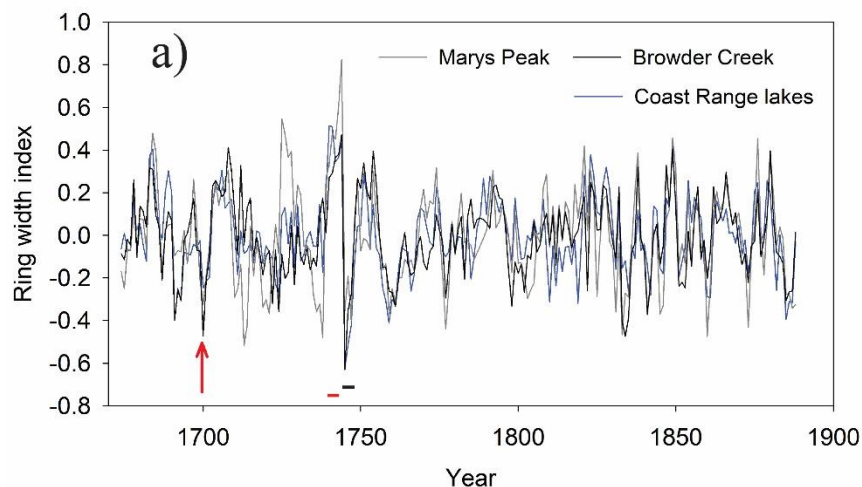


453

454

455 **Figure 4:** a) Tree-ring growth records of old-growth Douglas fir trees (*Pseudotsuga menziesii*) located in Mike Miller State  
456 Park, South Beach, Oregon (see **Figure 1**). Vertical axis shows ring growth in cm, time range covers several decades before  
457 and after AD 1700. The color of each growth record was relates to alpha-numeric labels of individual trees shown in legend,  
458 with location of trees shown in **Figure 3b**. Designation “A/B” represents two cores from same tree. Black arrow marks AD  
459 1700 date, red arrows highlight the AD 1691, 1738 and 1745 large growth reductions that may have been caused by a  
460 significant climatological events. (b) Shows detailed growth record of trees in (a) 4 years before and after 1700 (black arrow).  
461





462  
463

464 **Figure 5.** a) Difference in growth chronologies between Mike Miller and reference sites at Marys Peak, Browder Creek, and  
465 Oregon Coast Range lake sites. The A.D. 1700 chronology indicated by red arrow, the significant growth differences between  
466 coast and inland sites in 1739-1741 and 1745-1748 are highlighted by red and black lines, respectively. b) Shows location map  
467 with Marys Peak and lake sites relative to South Beach. The number of cores available at each site during the 1700 time period  
468 are South Beach (14), Marys Peak (28), Coast Range Lakes (31) and Browder Creek (30). The Oregon Coast Range lakes  
469 include: Beaver Dam Lake, Carlton Lake, Esmond Lake, Hamar Lake, Kauppi Lake, Klickitat Lake, Soup Lake, and Wasson  
470 Lake. Map created using digital elevation data points compiled by National Center for Environmental Information  
471 (<http://ncei.noaa.gov>)  
472